Extra encoding of fine grayscale data into 8-bit sRGB color space

Hisakazu Kikuchi, MEMBER SPIE
Hiroto Sato
Satoshi Hasebe
Naoki Mizutani
Shogo Muramatsu
Shigenobu Sasaki
Jie Zhou
Seishi Sekine
Niigata University
Department of Electrical and Electronic Engineering
Niigata 950-2181, Japan
E-mail: kikuchi@eng.niigata-u.ac.jp

Yoshito Abe
Dai Nippon Printing Company, Limited
Integrated Manufacturing Technology Laboratory
15-1 Kamiya 3-chome
Kita-ku, Tokyo 115-8611
Japan

Ikuo Tofukuji
Olympus ProMarketing Incorporated
Medical Informatics Department
3-4 Kanda Surugadai
Chiyoda-ku, Tokyo 101-0062
Japan

Makoto Nakashizuka
Tokyo University of Agriculture and Technology
Graduate School of Bio-Applications and Systems Engineering
2-24-16 Nakamachi
Koganei-shi, Tokyo 184-8588
Japan

Abstract. As an extra option, fine grayscale data that exceed eight bits per pixel are encoded into pseudogray colors in 8-bit sRGB color space to be displayed on an 8-bit sRGB CRT monitor. The characteristics of the pseudogray are investigated in terms of the CIELAB color difference and a^*b^* coordinates.
[DOI: 10.1117/1.1578492]

Subject terms: grayscale; pseudogray color; sRGB color system; color difference; CIELAB; CRT monitor.

Paper 020302 received Jul. 9, 2002; revised manuscript received Dec. 9, 2002; accepted for publication Dec. 30, 2002.

1 Introduction

10-bit and 12-bit grayscale images are used for some sophisticated applications[1–3] such as chest radiography, mammography, and computed radiography because of their rich ability in brightness discrimination. At present, a high-end monochrome CRT monitor for displaying those digital images typically costs ten thousand dollars. In contrast, a popular 24-bit color CRT monitor is quite cheap, while its display capability for grayscale data is limited to eight bits per pixel.

We describe a simple method to display the fine grayscale data into the sRGB color system[4,5] at the expense of small color difference. In addition, the characteristic data are presented for use by the public. Besides public use, for example, since teleradiology in real services is usually implemented in a personal computer-assisted environment, the authors believe that this study is one way to explore the possibility of general-purpose CRT monitors. Remember, however, that this work does not offer a complete substitution of high-end monochrome CRT monitors. Fine grayscale data is just imitated on 8-bit sRGB CRT monitors.

Our problem is finding a new approximate representation of fine gray in 9 bits or more in the 8-bit sRGB color system. The resulting pseudogray representation can be applied to the visualization on 8-bit sRGB CRT monitors. The less significant bits of a given grayscale data are mapped onto a particular point in the sRGB color space, so that the point may be located around the achromatic axis as close as possible.

The produced pseudogray in the sRGB color system is different from the true gray. It can be acceptable for some limited applications, unless the introduced chroma reaches a perceivable level, and if the pseudogray offers sufficient accuracy and linearity along the achromatic axis. To explore the possibility of its actual applications, several characteristics with respect to accuracy, linearity, and monotonic increase property are at first investigated. To give

 0091-3286/2003/$15.00

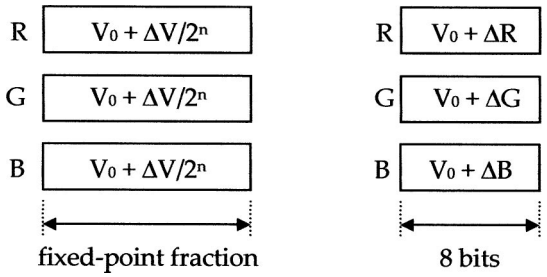

Fig. 1 Mapping between two 3-D vectors. A given grayscale value divided by 2^n (*left*) and its pseudogray (*right*) in the form of an RGB tristimulus vector encoded in 8 bits.

objective data for discussions and practical applications, we are going to compute the color difference between reference gray and the pseudogray and discuss them in the a^*b^* coordinates in CIELAB.[6–11]

Three options will be available to specify the fine fractional accuracy in the 8-bit sRGB color system. They are designed for 10- to 12-bit grayscale images. More importantly are two modes to match the pseudogray generation with the gamma correction performed in the imaging devices prior to encoding into digital data. The first is the legacy mode that works with traditional gamma corrected images. The other is the linear mode, and this is designed for gamma correction-free images such as x-ray pictures.

2 Pseudogray Mapping

2.1 *Mapping of Grayscale Data into sRGB*

A given grayscale image is assumed to be encoded with high accuracy that exceeds eight bits per pixel (bpp) in a particular RGB color system. The 8-bit accuracy is common to popular 24-bit color CRT monitors, and grayscale images in nine or more bpp cannot be displayed as they are, unless a simple truncation takes place as a preprocess. This is a mismatch between the grayscale information and a displaying device, and causes significant loss of information represented by fine tones in the grayscale.

A given $(n+8)$-bit grayscale value V can be expressed by

$$V=2^nV_0+\Delta V, \tag{1}$$

$$V_0=\mathrm{floor}[V/2^n], \tag{2}$$

where V_0 is the portion of the most significant 8 bits and ΔV represents the other less significant bits. Floor$[x]$ denotes the maximum integer that does not exceed x. The grayscale data are expressed by a 3-D vector

$$(V_0+\Delta V/2^n, V_0+\Delta V/2^n, V_0+\Delta V/2^n), \tag{3}$$

to be interpreted as an achromatic color in an RGB color space. Note that the row vector notation is used here to save space. The vector has identical entries and their value is a fractional number. This 3-D source vector is mapped onto a point in a 24-bit RGB color space as shown in Fig. 1. The corresponding destination vector is expressed by

$$(V_0+\Delta R, V_0+\Delta G, V_0+\Delta B), \tag{4}$$

where ΔR, ΔG, and ΔB are unknown integers.

The vector $(\Delta R,\Delta G,\Delta B)$ is a tuning vector to be added to the basement vector (V_0,V_0,V_0), so that the distance between the source and destination vectors are minimized in terms of a proper distance measure. Since the basement vector is common to the source and destination vectors, a possible approach to finding a solution is to minimize the distance between the tuning vector and the local source vector, $(1,1,1)\Delta V/2^n$, where the factor is a positive fraction smaller than unity. This is a kind of local optimization problem.

On the other hand, the tuning vector is an integer-weighted linear combination of three independent unit vectors. In addition, our problem is not simply to find separate tuning vectors, but to find a coordinated set of those vectors. For example, even if two tuning vectors, t_1 and t_2, have been found in such a way that they approximate two local source vectors, s_1 and s_2, respectively, it can be useless. It is the case if the lightness of t_1 is larger than that of t_2, and if s_1 is smaller than s_2 with respect to lightness. As long as the distance is defined in an encoding-discrete RGB color space, there is no hope in finding reasonable and acceptable solutions. We have to move on to another color space such as CIELAB where desirable conditions can be well defined.

As for global optimizations, any solution has to consider the mapping between the source vector of Eq. (3) and its destination vector of Eq. (4) rather than that between ΔV and $(\Delta R,\Delta G,\Delta B)$, since any color space available at present is nonuniform. Although a solution to this problem could be solved by an exhaustive search in the form of a one-to-one mapping table, such a solution would not be attractive for practical use because of its extensive storage space. Furthermore, a truly optimal solution has to match comprehensive conditions, including viewing conditions and visual appearance evaluated by the human visual system. This problem is too hard to be solved at present.

The challenge in this subsection is thus to find a set of 2^n integer-valued tuning vectors of $(\Delta R,\Delta G,\Delta B)$ to a fixed sequence between 0 and 2^n-1. At the beginning, to interpret a given grayscale value in terms of lightness, the RGB color system, where a given grayscale value has been encoded, must be defined. The standard default RGB color space, sRGB,[4,5] built for the Internet in 1999, is assumed in this work, because it is a nice compromise between device-dependent color spaces such as YIQ and YUV and device-independent color spaces such as CIEXYZ and CIELAB.[6–11] The transformation formulas from sRGB to CIEXYZ are defined as follows.[4,5]

$$X=0.4124R_s+0.3576G_s+0.1805B_s, \tag{5}$$

$$Y=0.2126R_s+0.7152G_s+0.0722B_s, \tag{6}$$

$$Z=0.0193R_s+0.1192G_s+0.9505B_s, \tag{7}$$

where X, Y, and Z are the CIE tristimulus values. The CIE chromaticity coordinates for ITU-R BT.709 reference primaries are as follows.

$$x=0.6400, \quad y=0.3300 \quad \text{for } R_s, \tag{8}$$

$$x=0.3000, \quad y=0.6000 \quad \text{for } G_s, \tag{9}$$

$$x=0.1500, \quad y=0.0600 \quad \text{for } B_s, \tag{10}$$

The standard illuminant white is CIE D_{65}, of which chromaticity is given by $x=0.3127$ and $y=0.3290$.

CIELAB is widely used to describe color difference in many industries. It is widely accepted as a standard interchange color space.[12] It is transformed from CIEXYZ as follows.[6–11]

$$L^*=116f(Y/Y_n)-16, \tag{11}$$

$$a^*=500[f(X/X_n)-f(Y/Y_n)], \tag{12}$$

$$b^*=200[f(Y/Y_n)-f(Z/Z_n)], \tag{13}$$

where

$$f(p)=p^{1/3} \quad \text{for } p>0.008856, \tag{14}$$

$$f(p)=7.787p+16/116 \quad \text{otherwise.} \tag{15}$$

L^* is referred to as lightness. a^* and b^* are referred to as redness-greenness and yellowness-blueness, respectively, and represent chroma components. X_n, Y_n, and Z_n are the tristimulus values of the standard illuminant.

The CIELAB color difference between two colors is defined as follows.[6–11]

$$\Delta E^*_{ab}=[(\Delta L^*)^2+(\Delta a^*)^2+(\Delta b^*)^2]^{1/2}, \tag{16}$$

where Δ stands for the difference between two quantities in issue.

In this way, once a given grayscale value V has been transformed onto a vector in CIELAB, then what has to be done is to find a mapping of the local source vector $(1,1,1)\Delta V/2^n$ to a tuning vector $(\Delta R_s, \Delta G_s, \Delta B_s)$ in the sRGB color space, so that both color and lightness differences between the true gray and the pseudogray may be tuned to zero as close as possible. To this end, an exhaustive search is applied for $n=4$ and a set of 16 vectors is found. The solution set of those vectors has to satisfy two additional conditions. That is, it has to keep the natural order correspondence to the integer sequence between 0 and 15. Second, the segmentation of the lightness scale has to be uniform as fine as possible. In other words, the bin sizes along the quantized lightness scale must be as regular as possible. The solution in 12-bit accuracy is listed in Table 1, where the lightness and color differences have been computed for a fixed basement, $V_0=25$. This value is equivalent to 10% of the full 8-bit range between 0 and 255. The values of color and lightness differences are valid for this basement value. If 11-bit accuracy is desirable, eight rows that are marked by a *single plus* in the rightmost column are taken away. If 10-bit accuracy is appropriate, the 4 rows marked with a double plus are furthermore suppressed, and only three vectors are left in the same order as they appear in the table. The null vector is not a tuning vector. It is merely included in the table for ease of understanding the endpoint mapping. It should be noted that the decimation of rows is not regular. This is a consequence of, on one hand, the nonlinear and nonuniform correspondence among color spaces in issue. On the other hand, the color difference is more significant than the accuracy in lightness in some of the practical applications intended.

Table 1 Tuning vectors for 12-bit grayscale data. The *plus*-marked eight rows are removed away in 11-bit accuracy. In addition, the four rows marked with double pluses are furthermore removed away in 10-bit accuracy. ΔL^* and ΔE^*_{ab} are valid to the basement value of $V_0=25$.

ΔV	ΔR_s, ΔG_s, ΔB_s	ΔL^*	ΔE^*_{ab}	Note
0	0, 0, 0	0.000	0.000	
1	0, 0, 1	−0.007	1.037	++
2	1, 0, −1	−0.011	1.276	+
3	1, 0, 0	−0.018	0.716	+++
4	1, 0, 1	−0.015	1.264	++
5	2, 0, −1	−0.029	1.773	+
6	1, 0, 2	0.013	2.177	+
7	2, 0, 0	0.009	1.420	+++
8	2, 0, 1	0.002	1.759	+
9	−1, 1, 1	−0.009	1.427	++
10	3, 0, 0	−0.009	2.113	+
11	−1, 1, 2	0.028	1.727	+
12	0, 1, 0	0.024	1.264	+++
13	0, 1, 1	0.018	0.708	+
14	0, 1, 2	0.011	1.222	++
15	1, 1, 0	0.007	1.033	+

Finally, a pseudogray color is computed by adding the common scalar value V_0 to the tuning vector $(\Delta R_s, \Delta G_s, \Delta B_s)$. Since the pseudogray color belongs to the 8-bit sRGB color space, it looks as if the number of gray levels had been augmented by a factor of the total number of tuning vectors.

Figure 2 shows the local mapping characteristics between grayscale values and the lightness values of the pseudogray. As seen in the plots, the monotonic increasing property between the grayscale value and the lightness of the pseudogray is satisfied as intended. Approximate linearity between them is also observed, while the bin size of quantization accuracy is nonuniform. It is worth noting that errors in both lightness and color differences vanish at two endpoints. The lightness of the pseudogray extends its value over the entire range between 0 and 255, and this mapping gamut is implemented by the basement integer V_0 added to the tuning vector. As a consequence, the global linearity and quantization accuracy are equally maintained over all unit intervals on the entire grayscale, where "unit" implies one digital count in 8-bit sRGB.

2.2 *Quantization and Gamma Correction of Given Grayscale Data*

Given grayscale data Q is assumed to have been encoded in $(n+8)$ bits, and the number of grayscale tones is thus 2^{n+8}. In contrast, the pseudogray has been produced by augmenting less significant n bits between successive two

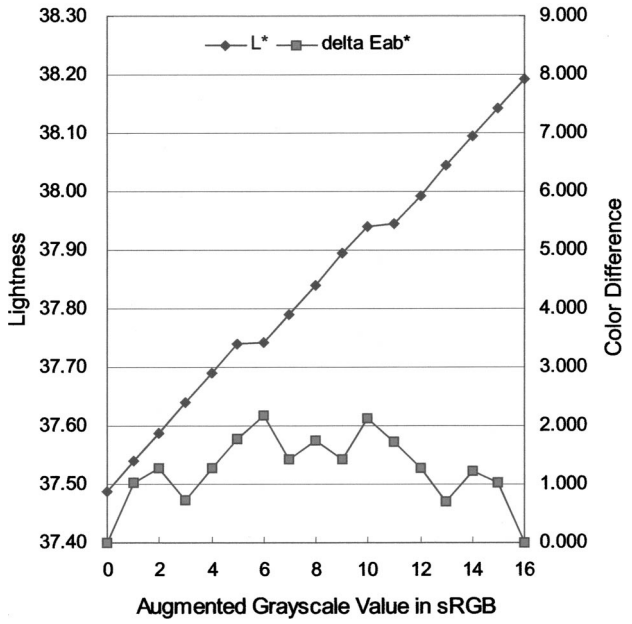

Fig. 2 Local mapping characteristics between the grayscale value and the pseudogray in 12-bit accuracy in terms of lightness and color differences. The basement value V_0 in the grayscale is 25. The grayscale value extends its range between 25 and 26 in digital counts, and the values along the horizontal axis should be read as those divided by 16.

tones in an 8-bit grayscale. The number of tones in the pseudogray is thus given by $255\times 2^n+1$, and differs from the number of gray levels in a given data. To solve this mismatch, a reduction in the number of tones is necessary, and a given grayscale data Q is quantized before its mapping to the pseudogray, as follows.

$$V=\mathrm{floor}[Q(2^8-1)2^n/(2^{n+8}-1)+0.5]. \tag{17}$$

The quantized grayscale data are mapped to the pseudogray by using the tuning vectors. Unfortunately, some tuning vectors cannot be applied at black and white ends, because any value outside [0,255] is impossible in 8-bit sRGB. In 12-bit accuracy, four pseudogray colors can have a negative value in R_s and B_s, and eight pseudograys can overflow beyond 255. These inhibited pseudograys are replaced by another admissible pseudogray of which lightness is closest to that of the inhibited pseudogray.

For the pseudogray to be evaluated, the reference gray has to be identified. It is hence appropriate to refer to the so-called gamma. A CRT monitor has a strong nonlinear transfer function between input and output. The output is proportional to γ'th power of the input, and γ is referred to as a CRT gamma or monitor gamma. Regarding the gamma, in-depth research is available in Refs. 13 and 14, where the device profile of a CRT monitor is described by the tone reproduction curves and transformation matrices. However, since the objective of this work is different from the precise characterization of CRT monitors, the term gamma is used in a sense similar to Refs. 4 and 5. A typical CRT gamma is 2.2 for sRGB[4,5] and NTSC.[6,15] The CRT gamma has to be corrected prior to displaying an image on CRT monitors. Most of cameras are thus designed to correct the CRT gamma, and hence most digital images have been gamma corrected and then encoded in digital data. This has been a legacy since the advent of television.[3–6,15]

In the sRGB color system, significant effort has been paid to the gamma,[4,5,12–14,16] and the viewing gamma is described by

$$\gamma_V=\gamma_C\gamma_D, \tag{18}$$

where γ_C and γ_D are the camera and display gammas. The display gamma is further factored into a product of look-up table and CRT gammas, and the former is recommended to be 1 and the latter is specified as 2.2. In accordance with the legacy and recent trends in color standardizations, a viewing gamma was defined as 1.125. As a result, a camera gamma is given by the reciprocal of 1.956.

The pseudogray can be directly applied to the legacy grayscale data. In the following description, the grayscale data encoded after a gamma correction of 2.2 are referred to as the legacy data, and linearly encoded data are referred to as linear data, which is a consequence of the camera gamma of unity.

To display those fine grayscale linear data on an 8-bit sRGB CRT monitor, the display gamma has to be corrected before the pseudogray mapping. When the viewing gamma for 8-bit sRGB CRT monitors and the display gamma are 1.125 and 2.2, respectively, the gamma-adjusted and quantized grayscale data for a given $(n+8)$-bit linear data Q is obtained by the following transformation.

$$V=\mathrm{floor}[(2^8-1)2^n q'+0.5], \tag{19}$$

where

$$q'=1.055q^{1/2.4}-0.055, \quad \text{for } q>0.00304, \tag{20}$$

$$q'=12.92q, \quad \text{otherwise}, \tag{21}$$

$$q=Q/(2^{n+8}-1), \tag{22}$$

and q is a normalized number between 0 and 1 by scaling of Q. Note that the discrepancy between 2.2 and 2.4 is due to an offset.[4,5] As a result of the gamma adjustment, the viewing gamma will be implemented by

$$\gamma_V=\gamma_C\gamma_A\gamma_D, \tag{23}$$

where γ_A is the adjusting gamma.

A sequence of the scaling, gamma correction, quantization, and pseudogray mapping is referred to as the linear mode, while a simplified process for the traditional gamma-corrected data is referred to as the legacy mode. These two modes are shown in Fig. 3, where square boxes illustrate data in respective formats. Upper and lower figures located at the left sides indicate the largest and smallest values of data.

Different types of CRT gammas can be treated in the same way. However, since the sRGB color system offers a common platform as a device-independent default standard at best at present, it is reasonable to limit our discussion in sRGB to a practical point of view.

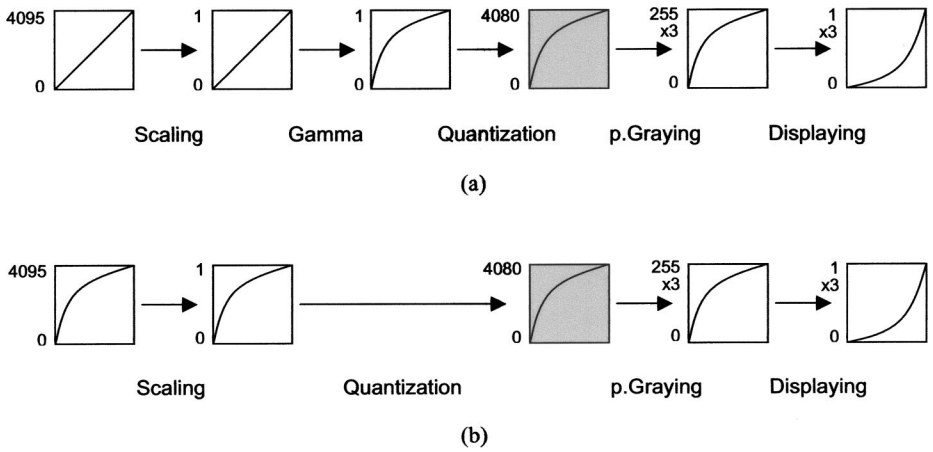

Fig. 3 (a) Linear mode and (b) legacy mode in 12-bit accuracy. The pseudogray is encoded into 8-bit sRGB and is decoded/displayed on an 8-bit sRGB CRT monitor so as to be evaluated in CIELAB. The reference gray for evaluations is marked by shaded squares.

2.3 *Numerical Evaluation of the Pseudogray*

The grayscale data quantized in $255\times 2^n+1$ tones is used as the reference gray in the present work. It is defined by the 8-bit sRGB encoded values after scaling, gamma adjustment, and quantization described in the previous section. The reference gray in 12-bit accuracy thus extends its value on the interval of $[0,4080]$ in 4081 levels. The reference gray is pretended by the pseudogray. This is referred to as nominal pseudogray to avoid confusion, and it has the same grayscale range as the reference gray, as listed in Table 2. Unfortunately, some impossible pseudogray colors can be computed as explained in the paragraph after Eq. (17) in the previous section. As a result of replacing those impossible pseudograys with admissible pseudogray colors, the net number of tones in the pseudogray colors will decrease to 4069, because there are four impossible pseudograys around the black end and eight impossible pseudograys around the white end. In summary, 4081 reference grayscale tones are pretended by 4081-level nominal pseudogray colors by using a total of 4069 admissible pseudogray colors. It should be noted that all evaluations in this work are performed on a virtual screen after decoding onto an 8-bit sRGB CRT monitor, where ''virtual'' implies numerical computations rather than experiments.

The color difference that is identical to the lightness difference between a given $(n+8)$-bit grayscale data and its reference gray has been examined for every tone for every viewing gamma among 1.0, 1.125, and 2.2. The maximum differences in lightness are listed in Table 3.

Table 2 Range of reference gray and pseudogray, and the number of available tones.

Accuracy	Value range: Given grayscale	Value range: Reference gray	Value range: Nominal pseudogray	Number of tones in the admissible pseudogray
10 bits	[0,1023]	[0,1020]	[0,1020]	1020
11 bits	[0,2047]	[0,2040]	[0,2040]	2038
12 bits	[0,4095]	[0,4080]	[0,4080]	4069

Note that the viewing gamma of 2.2 makes no sense for a viewing purpose, but it refers to the case when just the quantized data without any gamma adjustments are displayed on an 8-bit sRGB CRT monitor of $\gamma_D=2.2$. The maximum difference in lightness is 0.035 and 0.109 for 12- and 10-bit accuracy data, respectively.

Figure 4 shows the color and lightness differences between the reference gray and pseudogray over the whole range of the quantized grayscale in 10-bit accuracy for legacy data. The viewing gamma is assumed to be unity. The grayscale value extends its value 0 through 255, and the number of pseudogray colors plotted in the figure is 1021 in 10-bit accuracy. Hence the values in the horizontal axis can be a fraction such as 1/4, and the axis is referred to as the fractional grayscale in 8-bit sRGB. At a glance, one would see there are three plots for a single color difference, as well as for the lightness difference. However, it is not real. The upper three plots belong to the color difference,

Table 3 Maximum differences in lightness between a given grayscale data and the reference gray. $\gamma_V=2.2$ implies the case when just quantized data without any gamma corrections are displayed on an 8-bit sRGB CRT monitor of $\gamma_D=2.2$.

Accuracy	γ_V	γ_C	Max of $\lvert\Delta L^*\rvert$
12 bits	1.000	1/1.000	0.035
		1/1.956	0.035
		1/2.200	0.017
	1.125	1/1.000	0.033
		1/1.956	0.017
		1/2.200	0.034
	2.2*	1/1.000	0.017
10 bits	1.000	1/1.000	0.106
		1/1.956	0.109
		1/2.200	0.067
	1.125	1/1.000	0.107
		1/1.956	0.067
		1/2.200	0.099
	2.2*	1/1.000	0.067

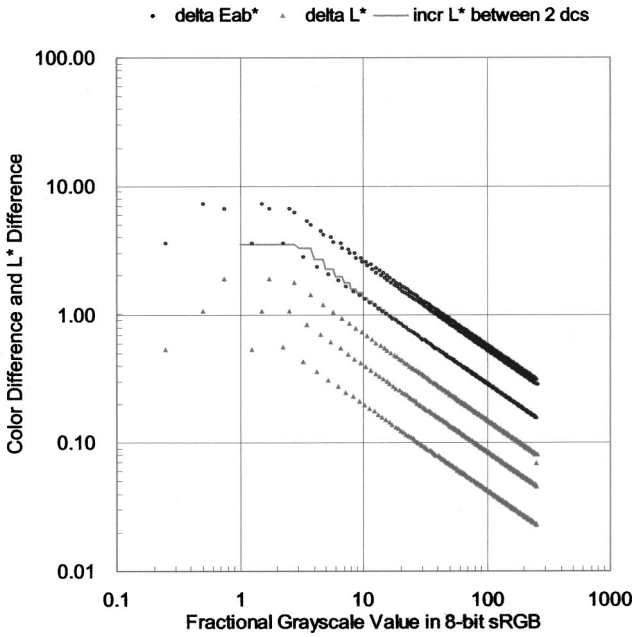

Fig. 4 Color difference (*upper*) and lightness difference (*lower*) in the case of 10-bit accuracy for legacy data. A unity viewing gamma is assumed. The thin line shows the incremental lightness between two successive digital counts in 8-bit sRGB. Triple split cluster plots are due to three tuning vectors for 10-bit accuracy.

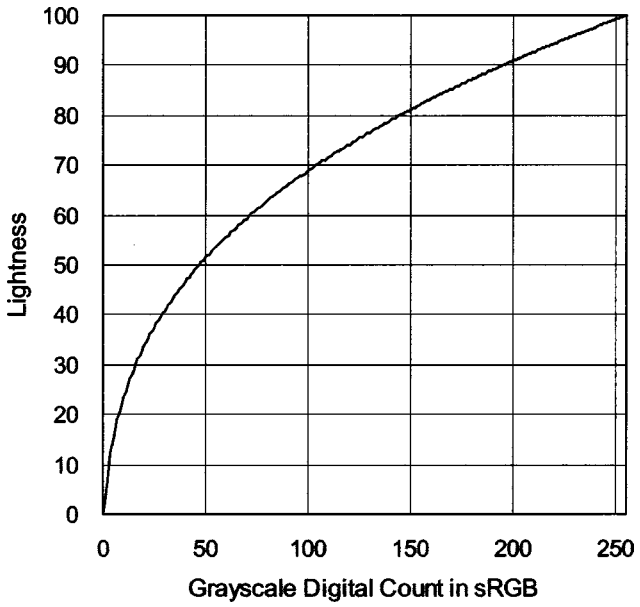

Fig. 5 Lightness versus 8-bit grayscale digital counts.

and the lower three plots belong to the lightness difference. Those split cluster plots are produced by the different error levels in three tuning vectors, whose behavior has been shown in Table 1 and Fig. 2. If successive points of a quantity in issue would be connected by line segments, those confusing split plots would not appear, but the mid-level plot would be completely hidden. A single point of ΔL^* is seen apart from its clusters at the white end in the figure. This is a consequence of the negotiated replacement of an inhibited tuning vector by an admissible one described in the previous section.

As observed in Fig. 4, both differences decrease as the grayscale value increases. This is a natural consequence, because the color difference behavior produced by the tuning vectors is identical in every unit interval along the grayscale and, at the same time, the lightness difference will decrease in proportion to the relative magnitude to the basement value. It is observed that the decreasing rate obeys the first-order derivative of the one third-power law between lightness and the *Y*-tristimulus value.

For reference purposes, drawn in the same figure is the thin line plot that shows the incremental lightness between two successive grayscale digital counts, rather than pseudogray colors, in 8-bit sRGB. Although the color difference is larger than the incremental lightness between two successive digital counts, the lightness difference of the pseudogray to the reference gray is surely smaller than this incremental lightness. The color difference of the pseudogray is approximately twice as large as the incremental lightness. This is a consequence of the fact that the pseudogray is approximated by the unity-spacing grids in the 8-bit sRGB color space at the expense of the intrinsic color difference in the achromatic color.

Although the color difference in Fig. 4 is large at the black end, it takes values smaller than unity over quite a broad range of the grayscale. In fact, the color difference is smaller than unity, when the 8-bit grayscale digital count exceeds 44, which is approximately equivalent to 49 in lightness. Figure 4 also shows that the color difference is smaller than 1.2 and 2.5, if the 8-bit digital count exceeds 32 and 11, respectively.

For ease of interpretation, the lightness dependency against the grayscale digital count is supplemented in Fig. 5. For the legacy data, 90% among the full dynamic range of the linear grayscale exceed the gamma corrected value of $0.351=0.1^{1/2.2}$ that is equivalent to the grayscale count of 89 among 255. As found in Fig. 4, this fact is restated as follows. For legacy 10-bit grayscale images, 90% of all gray values on the linear grayscale can be displayed on an 8-bit sRGB CRT monitor within the color difference of 0.62. This would be quite satisfactory, because it is hard to perceive such color differences smaller than 0.3, 0.6, 1.2, 2.5, or 3.0. The critical limit differs by literature,[3,6,7,10] and of course depends on the viewing conditions and the perceptual capability of individuals. It might be of significance to give a citation to typical values of average ΔE^*_{ab} in four commercial graphic CRT monitors: 0.63, 0.83, 0.97, and 1.90 are listed in Ref. 12.

The increasing plot in Fig. 6 shows the lightness of the pseudogray in 10-bit accuracy in 8-bit sRGB. The lower decreasing plot is the incremental lightness between two successive pseudogray colors in 10-bit accuracy. It looks as if two separate plots exist, but it is not true. As in Fig. 4, those split levels are just a result of irregular levels in lightness in the tuning vectors. The incremental lightness between two successive grayscale digital counts in 8-bit sRGB is also drawn in a mid-level thin line, once again the same as in Fig. 4. While the color difference represents the fidelity to the reference gray, the incremental lightness represents the smoothness in gradation in the pseudogray. It is smaller than unity except for only four colors around the

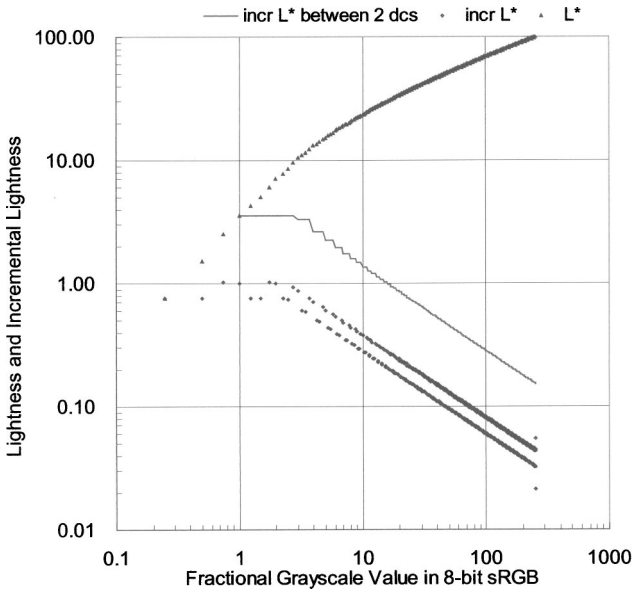

Fig. 6 Lightness and incremental lightness of the pseudogray in 10-bit accuracy.

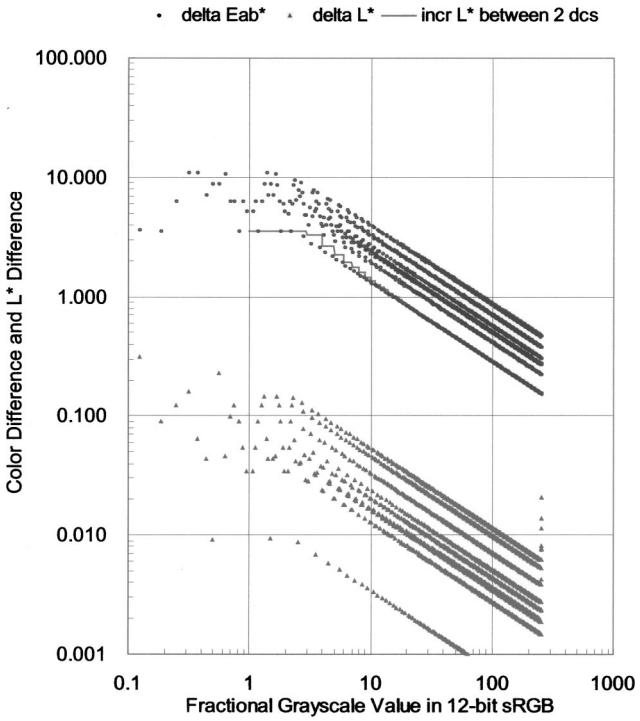

Fig. 7 Color difference (*upper*) and lightness difference (*lower*) in the case of 12-bit accuracy for legacy data. A unity viewing gamma is assumed. The thin line shows the incremental lightness between two successive digital counts in 8-bit sRGB.

black end. Therefore two successive pseudogray colors are expected to be perceived in a confusing gray, as far as the color difference from the reference gray is sufficiently small. The reason why there are two points of the incremental lightness apart from the major plot around the white end is because the replacement remedy for an inhibited tuning vector has been implemented.

Figures 7 and 8 show the results for 12-bit accuracy. All of the color difference, lightness difference, lightness, and incremental lightness in the 12-bit pseudogray colors show similar behaviors to those in 10-bit accuracy. In spite of the existence of a few disorders around the white end, the lightness difference and incremental lightness of the pseudogray surely remain lower than the incremental lightness between two successive grayscale digital counts in 8-bit sRGB, while the color difference is at a slightly higher level than that in 10-bit accuracy.

Another discussion is developed in terms of a^*b^* coordinates in CIELAB. Figure 9 plots the pseudogray colors in 12-bit accuracy. As seen in Fig. 9(a), the plots are classified in 15 clusters along respective converging linear plots that correspond to the 15 tuning vectors. The reason why only 12 converging linear clusters are seen in the plot is due to the geometric similarity in tuning vectors: three tuning vectors of (1,0,0), (2,0,0), and (3,0,0) are similar to each other. Also, (0,1,1) is similar to (0,2,2), which is produced by a sum of the tuning vector of $(-1,1,1)$ and a basement vector of (1,1,1). 15 tuning vector indices read from the leftmost column in Table 1 are given to 12 converging clusters in Fig. 9(a). A limited number of pseudogray colors, of which a digital count in 8-bit sRGB exceeds 45, are plotted in Fig. 9(b). Those pseudograys are found to concentrate within a considerably small area around the origin, and they number 3344, which amounts to 82% among 4081 nominal pseudogray colors.

3 Concluding Remarks

To explore the possibility in displaying fine grayscale images on 8-bit sRGB CRT monitors, pseudogray colors have been computed and their objective data have been pre-

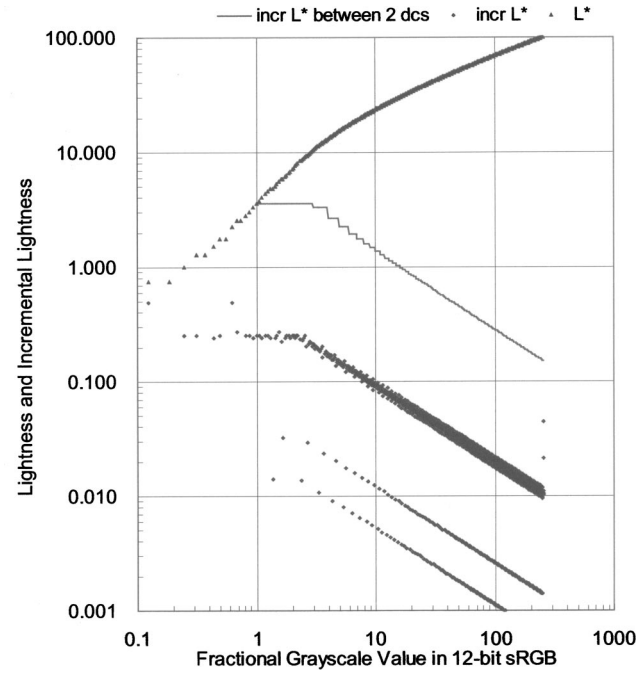

Fig. 8 Lightness and incremental lightness of the pseudogray in 12-bit accuracy.

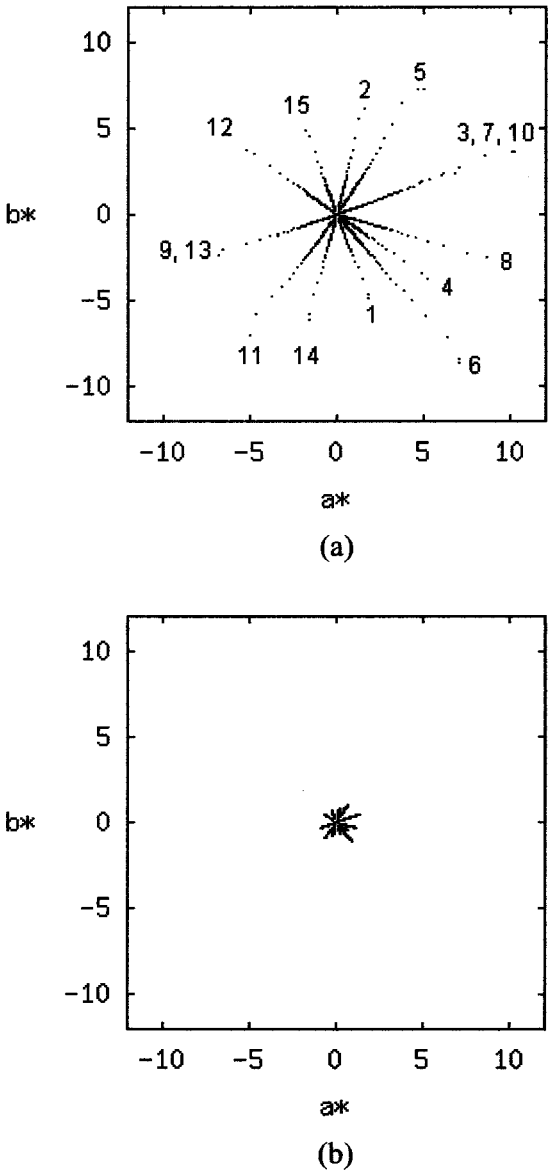

Fig. 9 Pseudogray colors of 12-bit accuracy in a^*b^* coordinates: (a) the whole plot for all pseudogray colors, and (b) a plot for the pseudogray colors brighter than 50 in lightness.

sented in terms of CIELAB color difference and a^*b^* coordinates. Two modes are available for treating gamma-corrected and linear data both in the 8-bit sRGB color space. Three options in quantization accuracy have been designed for use with 10-, 11-, and 12-bit grayscale data.

A global optimization of color mapping between the grayscale data and its pseudogray is an unsolved problem at present. Nevertheless, the described pseudogray can be sufficiently useful in some limited but real applications.

Acknowledgments

The authors would like to express their sincere thanks to Professors Kunio Sakai and Kotaro Okamoto of the School of Medicine, Niigata University, for their valuable comments and chest radiographic images. This work has been partly supported by a grant given by Hitachi Unisia Automotive and a five-year project granted by Telecommunications Advancement Organization of Japan. The authors would like to thank Dr. Naoya Katoh, Sony Corporation, for his provision of valuable Refs. 12–14.

References

1. H. Kobatake, "Mammography database," *Med. Imaging Technol.* **13**(3), 267–270 (1995).
2. *Mammography database*, Inst. of Computer-Assisted Diagnosis of Medical Images, Tokyo (1995).
3. *Handbook of Image and Video Processing*, A. Bovik, Ed., Academic Press, San Diego, CA (2000).
4. M. Stokes, M. Anderson, S. Chandrasekar, and R. Motta, "A standard default color space for the internet—sRGB," (1996), http://www.w3.org/Graphics/Color/sRGB.html.
5. IEC61966-2.1, "Default RGB colour space—sRGB," 100/PT61966 (PL) 34 (1998).
6. J. Yamauchi and T. Kanazawa, *Handbook of Color Science*, Nihon Shikisai-gakkai, Ed., University of Tokyo Press, Tokyo (1980).
7. Y. Nayatani, *Industrial Color Science*, Asakura Shoten, Tokyo (1980).
8. G. Wyszecki and W. S. Stiles, *Color Science: Concepts and Methods, Qualitative Data and Formulae*, 2nd ed., John Wiley and Sons, New York (1982).
9. S. Ando and S. Sekine, *Optical Engineering*, IPC Press, Tokyo (1991).
10. Y. Miyake, *Analysis and Evaluation of Digital Color Images*, University of Tokyo Press, Tokyo (2000).
11. N. Ohta, *Color Engineering*, 2nd ed., Tokyo Denki University Press, Tokyo (2001).
12. N. Katoh, K. Nakabayashi, M. Ito, and S. Ohno, "Effect of ambient light on the color appearance of softcopy images: Mixed chromatic adaptation for self-luminous displays," *J. Electron. Imaging* **7**(4), 794–806 (1998).
13. N. Katoh, T. Deguchi, and R. S. Berns, "An accurate characterization of CRT monitor (I) verifications of past studies and clarifications of gamma," *Opt. Rev.* **8**(5), 305–314 (2001).
14. N. Katoh, T. Deguchi, and R. S. Berns, "An accurate characterization of CRT monitor (II) proposal for an extension to CIE method and its verification," *Opt. Rev.* **8**(5), 397–408 (2001).
15. *Handbookbook of Television and Image Information Engineering*, ITE, Ed., Ohm-sha, Tokyo (1990).
16. N. Katoh, "Practical method for appearance match between soft copy and hard copy," *Proc. SPIE* **2170**, 170–181 (1994).

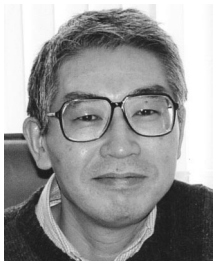

Hisakazu Kikuchi received his BE and ME degrees from Niigata University, Japan, in 1974 and 1976, respectively, and the DE degree in electrical and electronic engineering from Tokyo Institute of Technology in 1988. In 1976 he worked at Information Processing Systems Laboratory, Fujitsu Limited, Tokyo, for three years. Since 1979 he has been with Niigata University, where he is a professor in the Department of Electrical Engineering. From 1992 to 1993, he was a visiting scholar at the electrical engineering department of the University of California, Los Angeles. His research interests include digital signal processing, image/video processing, and wavelets as well as spread spectrum communication systems. He is a member of SPIE, IEEE, the Institute of Electronics, Information and Communication Engineers, the Institute of Image Information and Television Engineers of Japan, Japan SIAM, the Research Institute of Signal Processing, and the Society of Computer-Assisted Diagnosis of Medical Images.

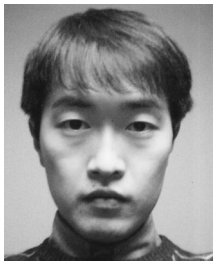

Hiroto Sato received his BE and ME degrees from Niigata University in 2000 and 2002, respectively. He currently works at Digital Media Network Company, Toshiba Corporation, Tokyo. His research interests include image processing, network technology, and wireless communications.

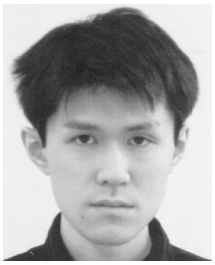

Satoshi Hasebe received his BE and ME degrees from Niigata University in 2000 and 2002, respectively. He is currently a PhD candidate at Niigata University. His research interests include digital signal processing, image/video processing, and wavelets.

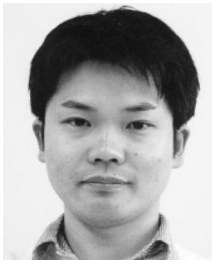

Naoki Mizutani received his BE and ME degrees from Niigata University, Japan, in 1999 and 2001, respectively. He is currently a PhD candidate at Niigata University. His research interests are in the area of digital signal processing and image processing.

Shogo Muramatsu received the BE, ME, and DE degrees in electrical engineering from Tokyo Metropolitan University in 1993, 1995, and 1998, respectively. In 1997, he joined Tokyo Metropolitan University, Tokyo. Since 1999 he has been with Niigata University, where he is an associate professor in the Department of Electrical and Electronic Engineering. His research interests are in digital signal processing, multirate systems, image processing, and VLSI architecture. He is a member of IEEE, the Institute of Electronics, Information and Communication Engineers, the Information Processing Society of Japan, and the Institute of Image Information and Television Engineers.

Shigenobu Sasaki received his BE, ME, and PhD degrees from Nagaoka University of Technology, Japan, in 1987, 1989, and 1993, respectively. Since 1992, he has been with Niigata University, where he is an associate professor at the Department of Electrical and Electronic Engineering. From 1999 to 2000, he was a visiting scholar at the Department of Electrical and Computer Engineering, University of California, San Diego. His research interests are in the areas of digital communications with special emphasis on spread spectrum communication systems and wireless communications. He is a member of IEEE, the Institute of Electronics, Information and Communication Engineers, and the Society of Information Theory and its Applications, Japan.

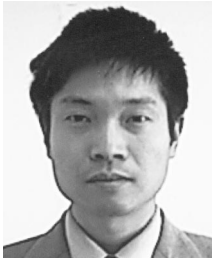

Jie Zhou received his BE and ME degrees from Nanjing University of Posts and Telecommunications, China, in 1985 and 1990, respectively, and received the PhD degree in computer science and telecommunications, Gunma University, Japan, in March 2001. He joined Chongqing University of Posts and Telecommunications in 1990, where he is an associate professor. Since April 2001, holding the professorship, he has also been with the Department of Electrical and Electronic Engineering, Niigata University, Japan, where he currently serves as a research associate. His research interests lie in the areas of cellular networks, signal processing, and radio wave propagation in mobile communications.

Seishi Sekine received his BE and ME degrees in electrical engineering from Niigata University in 1964 and 1966, respectively, and the DE degree from the Tokyo Institute of Technology in 1985. Since 1965 he has been with Niigata University, where he is a professor in the Department of Biocybernetics. His research interests are in the areas of illuminant measurement, holography, and optical computing. He received a Research Award and Achievement Award from the Illuminating Engineering Institute of Japan (IEI-J) in 1977 and 1995, respectively. He is a fellow of IEI-J and a member of the Color Science Association of Japan, Laser Society of Japan, Society of Japan Applied Physics, IEICE, and IEEJ.

Yoshito Abe received the degrees of BE, ME, and PhD all in electronic engineering from Niigata University in 1985, 1988, and 1998, respectively. In 1985, he worked at the Research and Development Center, Nemic-Lambda K. K., Nagaoka-shi. In 1988, he joined Dai Nippon Printing Company, Limited, Tokyo, where he is now a senior researcher in the Integrated Manufacturing Technology Laboratory. His research interests are in digital signal processing, image processing, and parallel computing. He is a member of the IEICE, ITEJ and Imaging Society of Japan.

Ikuo Tofukuji received his BE and ME degrees in electrical engineering from Niigata University, Japan, in 1974 and 1976, respectively. Since he joined Olympus Optical Company, Limited, Tokyo, in 1976, he has been with research and development in the areas of instrumentation and medical engineering including blood analyzers, telepathology systems, and optical memory cards, and is now a chief manager of the medical informatics department, Olympus ProMarketing Incorporated, Tokyo. He serves as a board member of the Japanese Society for Telepathology and Pathology Informatics, chairperson of Healthcare Systems Committee of Japanese Society of Healthcare Systems Industry (JAHIS) in Tokyo, a member of the Healthcare Coordination Strategy Committee of Ministry of Health, Labor and Welfare, Japan, and a is a member of the Telepathology Committee of Medical Information Systems Development Center (MEDIS-DC) in Tokyo. Also, he is a PhD student at Niigata University. His research interests are in the areas of telemedicine, and international standardizations and cooperation in medical engineering.

Makoto Nakashizuka received his BE, ME, and PhD degrees from Niigata University in 1988, 1990, and 1993, respectively. He was with the Department of Information Engineering, Niigata University, as a Research Associate from 1993 to 1997. He is now an associate professor at the Graduate School of Bio-Applications and Systems Engineering, Tokyo University of Agriculture and Technology. His research interests include time-scale/frequency analysis and its applications to signal, biomedical, vision, and image processing. He is a member of IEEE, IEICE, the Institute of Image Information and Television Engineers, and the Institute of Image Electronics Engineers of Japan.